

# Direct measurement of plowing friction and wear of a polymer thin film using the atomic force microscope

Binyang Du

*State Key Laboratory of Polymer Physics and Chemistry, Changchun Institute of Applied Chemistry, Chinese Academy of Sciences, Changchun, Jilin, 130022, People's Republic of China*

Mark R. VanLandingham

*Building and Fire Research Laboratory, National Institute of Standards and Technology, 100 Bureau Dr. Stop 8621, Gaithersburg, Maryland 20899-8621*

Qingling Zhang and Tianbai He<sup>a)</sup>

*State Key Laboratory of Polymer Physics and Chemistry, Changchun Institute of Applied Chemistry, Chinese Academy of Sciences, Changchun, Jilin, 130022, People's Republic of China*

(Received 10 July 2000; accepted 5 March 2001)

Nanometer-scale plowing friction and wear of a polycarbonate thin film were directly measured using an atomic force microscope (AFM) with nanoscratching capabilities. During the nanoscratch tests, lateral forces caused discrepancies between the maximum forces for the initial loading prior to the scratch and the unloading after the scratch. In the case of a nanoscratch test performed parallel to the cantilever probe axis, the plowing friction added another component to the moment acting at the cantilevered end compared to the case of nanoindentation, resulting in an increased deflection of the cantilever. Using free-body diagrams for the cases of nanoindentation and nanoscratch testing, the AFM force curves were analyzed to determine the plowing friction during nanoscratch testing. From the results of this analysis, the plowing friction was found to be proportional to the applied contact force, and the coefficient of plowing friction was measured to be  $0.56 \pm 0.02$ . Also, by the combination of nanoscratch and nanoindentation testing, the energetic wear rate of the polycarbonate thin film was measured to be  $0.94 \pm 0.05 \text{ mm}^3/(\text{N m})$ .

## I. INTRODUCTION

As polymers become more widely used as bearing and sliding materials, their friction and wear properties become of greater interest and importance. Understanding the mechanisms and basic principles of polymer wear is essential for maximizing the life of polymer products such as the compact disc, which is made of polycarbonate (PC). Recent developments in atomic force microscopy (AFM) and depth-sensing indentation (DSI) allow for the study of tribology on the scale of nanometers, thus enabling new understanding of the origins of friction, adhesion, wear, and lubrication.<sup>1</sup> For example, both AFM and DSI have been used to measure mechanical properties, such as hardness and elastic modulus, of materials using nanoscale indentation<sup>2-4</sup> and to investigate the scratch resistance of diamond-like carbon coatings using nanoscale scratch and wear testing techniques.<sup>5-8</sup> However, only in a few instances<sup>3,9</sup> has the indentation and scratch behavior of polymeric materials been studied with submicrometer spatial resolution.

The scratch resistance of materials has been characterized only qualitatively or semiquantitatively using AFM due to unknown torsional spring constants of the AFM probe, which leads to unknown lateral forces during scratching.<sup>5-8</sup> In general during an AFM scratch test, the probe tip moves toward the sample, contacts and penetrates into the sample surface, moves laterally across the sample, and then lifts off of the sample surface. Concurrently, deflection of the cantilever probe is measured, often by using an optical lever system. The individual scratch created on the surface can then be imaged and the surface damage can be characterized.<sup>9</sup> As is the case during AFM indentation, a force plot of the cantilever deflection versus the displacement in the  $z$  direction is also recorded. Unlike AFM indentation studies,<sup>3</sup> however, the force plot has not been utilized in scratching studies to characterize the mechanical behavior of the material. This lack of use might be because the force plot is recorded not during the scratch but rather while the tip is moving toward and away from the sample at the start and end of the scratch, respectively.<sup>10</sup> In this work, force plots for AFM scratch tests are compared to those of AFM indentation for a diamond-tipped AFM probe

<sup>a)</sup>Address all correspondence to this author.  
e-mail address: tbhe@ns.ciac.jl.cn

and a PC thin-film sample. By movement of the probe parallel to the cantilever axis during scratching, the known bending spring constant of the probe is used to calculate applied normal and lateral forces using the measurement of tip deflection in the force plot. Through a mechanics analysis of quasi-static forces acting on the AFM probe tip during scratching, the plowing friction force is calculated and used to estimate the coefficient of friction for the diamond tip–PC system. The energetic wear rate of PC is also estimated from the surface deformation measured in indentation and scratch tests.

## II. EXPERIMENTAL

AFM indentation and scratch tests were performed using a multimode scanning probe microscope and NanoScope IIIa controller (Digital Instruments) with a diamond tip mounted on a stainless steel cantilever (Digital Instruments). The diamond tip was a three-sided pyramid with an apex angle of about  $60^\circ$  (manufacturer's specification<sup>10</sup>), and the spring constant of the stainless steel cantilever was measured by the manufacturer to be  $186 \text{ N/m} \pm 11 \text{ N/m}$  (here and throughout the text, the numeric value following a  $\pm$  symbol is the estimated standard deviation for the corresponding measurement). The cantilever sensitivity was measured using a sapphire sample before and after the indentation and scratch tests following procedures described elsewhere.<sup>3,11</sup> For all AFM indentation and scratch tests, the  $z$  scan rate was 4 Hz and the lateral compensation angle was  $25^\circ$ . The proper lateral compensation angle was determined using methods detailed elsewhere<sup>11</sup> (also, see the Results and Discussion section). For the scratch tests, single-pass, unidirectional scratching was performed using a scratch length of approximately 600 nm and a scratch rate of approximately 0.5 Hz. Also, for the majority of scratch tests, the scratch angle was set as  $0^\circ$  (parallel to the cantilever axis) unless otherwise indicated. The sample used was a bisphenol-A–polycarbonate thin film with an estimated thickness of approximately  $10 \mu\text{m}$ . This sample was prepared by mixing a solution with a mass fraction of 0.02 of the polymer in tetrahydrofuran (THF) followed by casting onto freshly cleaved mica. To ensure low surface roughness and evaporation of the solvent, the thin film was annealed in vacuum for several days at  $120^\circ\text{C}$ . The surface roughness  $R_q$  of the sample was less than 1 nm as measured from  $10 \mu\text{m} \times 10 \mu\text{m}$  topographic AFM images.

## III. RESULTS AND DISCUSSION

### A. Force plot analysis

Normally, AFM scratch tests are performed such that the AFM probe moves laterally across the sample perpendicular (scratch angle =  $90^\circ$ ) to the cantilever

axis.<sup>9,10</sup> An alternative method is to move the probe parallel (scratch angle =  $0^\circ$ ) to the cantilever axis. In the former case, the torsional response of the probe can be directly measured during scratching. However, the torsional spring constant of the probe is generally not known and is extremely difficult to measure, and thus, the frictional forces during scratching are unknown. In the latter case, normal and frictional forces will both result in bending of the probe, making separating the two effects difficult. However, the bending probe spring constant can be measured and is known in the current study.

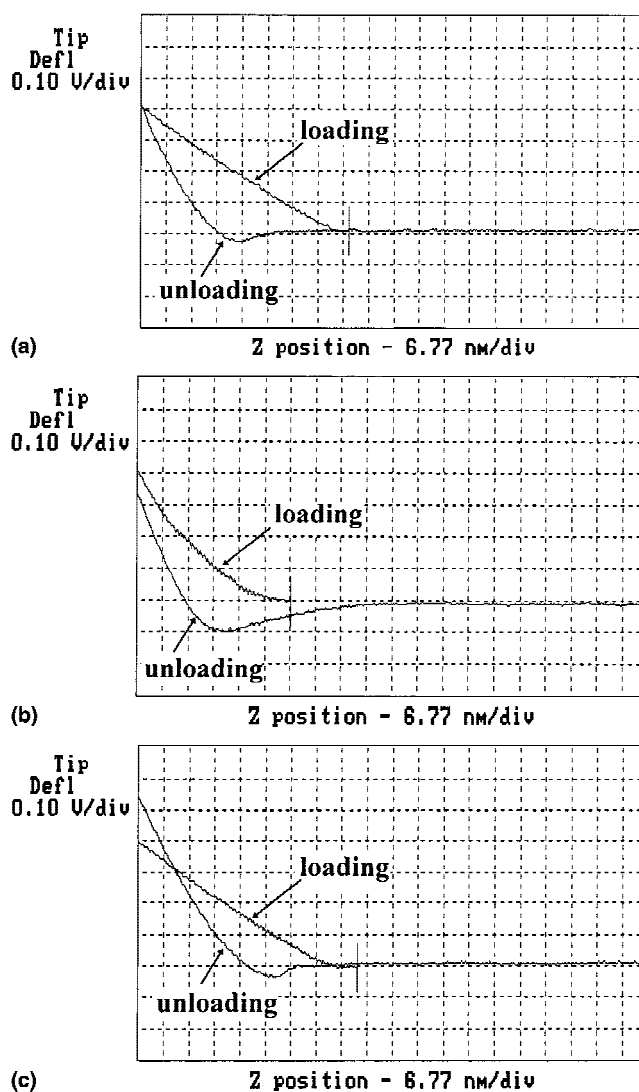


FIG. 1. AFM force plots for the diamond-tipped AFM probe on a PC thin film for (a) nanoindentation, (b) nanoscratching with a scratch angle of  $90^\circ$ , and (c) nanoscratching with a scratch angle of  $0^\circ$ . For each experiment, the same loading tip deflection was used, and the  $z$  scan rate and lateral compensation angle were 4 Hz and  $25^\circ$ , respectively. For the nanoscratch tests, the scratch length was approximately 600 nm and the scratch rate was approximately 0.5 Hz.

In Fig. 1, three typical force plots are shown, one for nanoindentation and the other two for nanoscratching with scratch angles of  $90^\circ$  and  $0^\circ$ , respectively. Distinct differences were observed between these types of force plots that are related to the differences in the tests themselves. As discussed previously, a force plot is a record of the cantilever deflection versus the displacement in the  $z$  direction of the tip relative to the sample. Further, no feedback is utilized to control applied forces or displacements. Only a maximum cantilever deflection is prescribed that will be achieved at the end of the initial loading of the sample. For an indentation force plot, the tip approaches the sample, achieves contact with the sample, loads to the prescribed maximum cantilever deflection, and immediately unloads the sample. Thus, the maximum cantilever deflection is nominally the same for loading and unloading, as shown in Fig. 1(a).

For scratch tests, the initial loading to the maximum cantilever deflection is recorded, followed by lateral motion of the tip to create the scratch and then followed by unloading of the sample. The occurrence of the scratch event between the recording of the load and unload events combined with a lack of force feedback often can lead to differences between the maximum cantilever deflections for the loading and unloading force curves. For example, for a scratch angle of  $90^\circ$ , the maximum cantilever deflection was smaller for unloading (i.e., after scratching) than for the initial loading prior to scratching, as shown in Fig. 1(b). This decrease could be due to cross talk between the vertical and lateral cantilever displacement signals of the optical lever system and/or to a nonlevel surface relative to the AFM scanner, such that the height of the probe relative to the sample surface increased during scratching. For a scratch angle of  $0^\circ$ , the maximum cantilever deflection was larger after scratching than for the initial loading prior to scratching, as shown in Fig. 1(c). While this change could also be affected by a nonlevel sample, measurements were made with different samples in various orientations relative to the AFM without any discernible effect on the force plots. Therefore, the measured increase in cantilever deflection after scratching should be related directly to lateral surface forces created during scratching.

Assuming the forces acting on the AFM cantilever probe during scratching to be essentially quasi-static, a mechanics analysis was performed for a scratch angle of  $0^\circ$ . In Fig. 2, free-body diagrams are shown for an AFM probe for the cases of an applied normal force only [Fig. 2(a)], an indentation test [Fig. 2(b)], and a scratch test with a scratch angle of  $0^\circ$  [Fig. 2(c)]. For an idealized indentation test [Fig. 2(a)], the only tip-sample interaction force is the normal force,  $P$ . While  $P$  results in a vertical displacement of the probe tip, the bending of the cantilever also causes a lateral displacement of the probe tip.<sup>11</sup> Because the tip-sample contact is not frictionless, in general, the probe tip is constrained from lateral motion and a corresponding lateral force,  $F_L$ , is created, as shown in Fig. 2(b). The AFM software allows a compensating lateral motion of the probe to be applied that is proportional to the vertical motion of the probe during indentation.<sup>10,11</sup> The actual probe motion is then at an angle, called the lateral compensation angle, to the  $z$ -axis of the system, and the lateral component of this motion results in a compensating force,  $F_c$ . The compensating force,  $F_c$ , completely counteracts the lateral force,  $F_L$ , when the two forces are equal in magnitude and opposite in direction, and the ideal indentation case shown in Fig. 2(a) results. In practice, total compensation is difficult to achieve, so the objective of lateral compensation becomes one of minimizing experimental uncertainties and, hence, minimizing the additional moment term at the cantilevered end.

For the case of a scratch test with a scratch angle of  $0^\circ$ , an additional friction force,  $f$ , occurs due to the lateral displacement of the probe across the sample surface with a tip-sample normal force,  $P$ . The lateral reaction force at the cantilevered end is equal in magnitude and opposite in direction to the vector resultant of  $f$ ,  $F_c$ , and  $F_L$ . Ideally,  $F_L = F_c$ , or at least the difference is small, such that  $f$  is the only significant lateral force acting on the probe tip. In any case, the resulting lateral reaction force acting on the probe tip yields an additional term,  $M_f$ , to the moment  $M$  compared to the case of idealized indentation [compare Figs. 2(a) and 2(c)]. This additional moment term will cause the deflection of the cantilever after scratching to be larger than before scratching, as was observed experimentally and is shown in Fig. 1(c). Assuming that the difference between  $F_c$  and  $F_L$  is negligibly

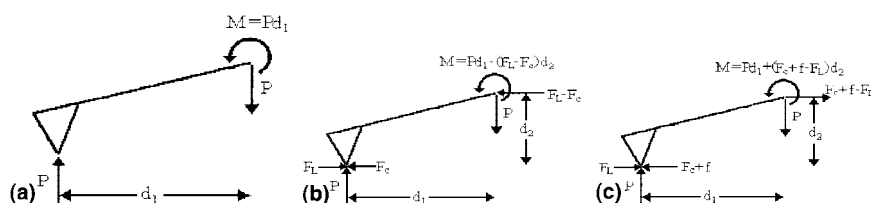


FIG. 2. Free-body diagrams of the AFM cantilever probe for (a) a normal force,  $P$ , applied to the probe tip (idealized indentation), (b) forces applied during indentation testing, and (c) forces applied during nanoscratch testing with a scratch angle of  $0^\circ$ .

small,  $M_f$  can be expressed as  $M_f = fd_2$ , where  $d_2$  is the vertical distance between the probe tip and the cantilevered end. However, the optical lever system of the AFM measures tip deflection, which is most easily converted to a force,  $P$ , through the bending spring constant of the cantilever. To determine  $f$  experimentally, the measured change in tip deflection or, equivalently, force,  $\Delta P$ , is related to  $M_f$  through the equation  $M_f = \Delta Pd_1$ , where  $d_1$  is the horizontal distance between the probe tip and the cantilevered end. In other words, the addition of a friction force  $f$  to the idealized indentation case of Fig. 2(a) adds an equivalent moment term, i.e. causes an equal increase

in cantilever bending, as an increase,  $\Delta P$ , in the normal force through the moment arm  $d_1$ . Thus,  $f = \Delta Pd_1/d_2$ . For the particular indentation cantilever probe used in this study, the angle of the cantilever to the horizontal was  $12^\circ$ , the length and thickness of the cantilever were approximately 350 and 13  $\mu\text{m}$  and 264 and 173  $\mu\text{m}$ , respectively, and the diamond tip extended approximately 100  $\mu\text{m}$  beneath the underside of the cantilever. Using these probe dimensions,  $d_1$  and  $d_2$  were calculated from simple geometry to be 264 and 173  $\mu\text{m}$ , respectively, for which the cantilever thickness of 13  $\mu\text{m}$  was neglected.

## B. Nanoscratch tests of PC

In Fig. 3, a series of scratches on a PC thin film is shown for seven different contact force levels. At the starting end of each scratch, the surface deformation was consistent with the triangular pyramidal shape of the tip, while, at the completion end of each scratch, wear debris was piled up. Increasing the scratch force increased the amount of wear debris, indicating that more material was displaced by the diamond tip for larger contact forces. Using the corresponding force plots recorded during nanoscratch testing, the plowing friction force ( $f$ ) was measured as a function of the contact (scratch) force ( $P$ ). As shown in Fig. 4, the plowing friction was proportional to the scratch force. The coefficient of plowing friction,  $\mu$ , between the diamond tip and the PC film was calculated from the slope of the fitted linear curve to be  $0.56 \pm 0.02$ .

A polymeric thin film can respond to forces exerted during a scratch in one of three ways, viscoelastic deformation, viscoplastic deformation, or fracture. Mechanical measurements using the AFM, however, can only discern between recoverable deformation and unrecoverable deformation. For AFM indentation measurements, deformation recovered in the time scale of the measurement is generally taken to be elastic deformation, while

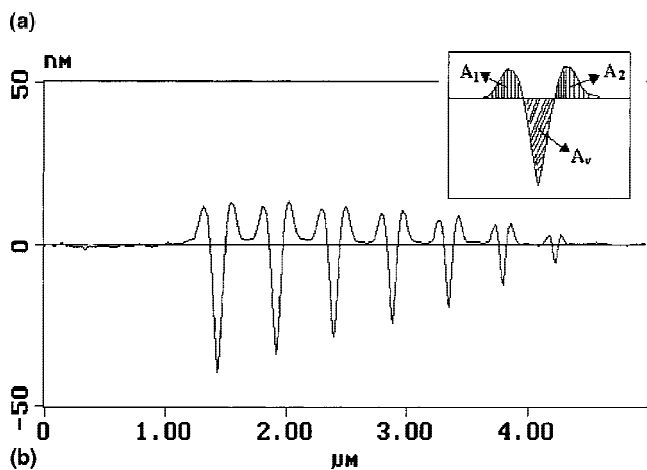
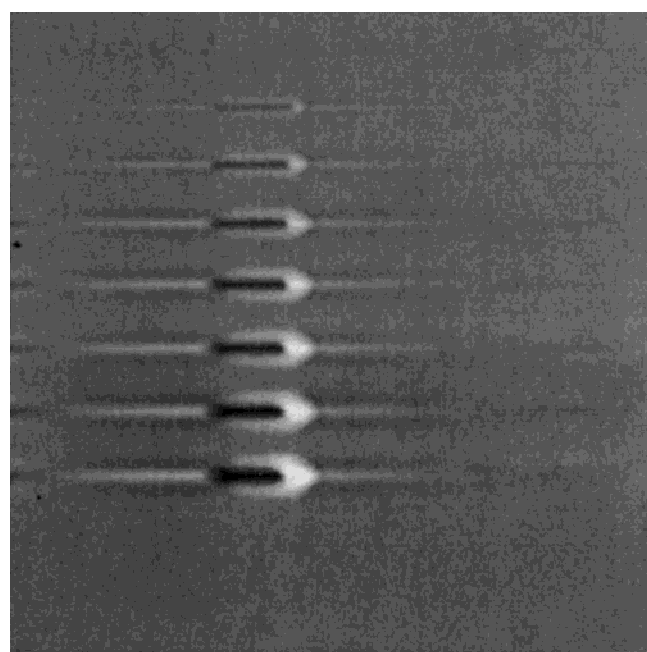


FIG. 3. (a) The  $5 \mu\text{m} \times 5 \mu\text{m}$  topographic AFM image of a series of scratches on a PC thin film made using seven different contact force levels and (b) a cross-sectional profile of the seven scratches taken using the AFM topographic data. The scratch length was approximately 600 nm, and the scratch rate was approximately 0.5 Hz. The scratches and the image were made using the same diamond-tipped AFM probe.

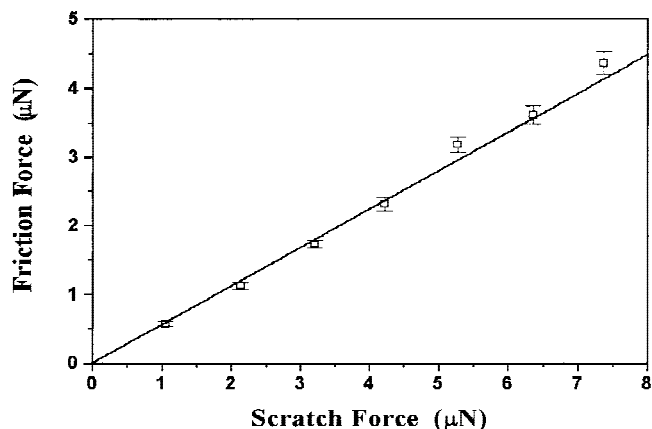


FIG. 4. Plot of the plowing friction force as a function of the normal contact (scratch) force for the diamond-tipped AFM probe scratching a PC thin film.

deformation not recovered in the time scale of the measurement is generally taken to be plastic deformation. In Fig. 5, AFM indentation measurements of elastic, plastic, and total deformation of the PC thin film are shown for the same normal force levels applied in the nanoscratch tests. From these results, the elastic deformation appears to play an important role for nanometer-scale contact involving polymer thin films. Intuitively, wear is likely to be much lower in conditions of elastic rather than plastic deformation.

From the cross sections of the scratches shown in Fig. 3(b), the cross-sectional area  $A_v$  for the scratch appears to be similar to the sum of the cross-sectional areas  $A_1$  and  $A_2$  for the material piled up next to the scratch. According to Jones *et al.*,<sup>9</sup> the similarity of these areas indicates that the permanent deformation created during scratch was dominated by plastic deformation and not fracture. For the case in which all the material displaced by the indenter tip is removed as wear debris, the energetic wear rate  $K_e$ , which is the volume  $V$  of material displaced per unit work of friction, can be given as<sup>12</sup>

$$K_e = \frac{V}{fL} = \frac{A_v L}{fL} = \frac{A_v}{f}, \quad (1)$$

where  $A_v$  is the cross-sectional area of a wear groove and  $V$  is the volume of material removed when the indenter scratches the sample over a distance  $L$ . However, an appreciable proportion of material was merely displaced plastically to the edges of the groove. In a single scratch experiment, the fraction of material removed as wear debris,  $f_{ab}$ , can be described by

$$f_{ab} = \frac{A_v - (A_1 + A_2)}{A_v}, \quad (2)$$

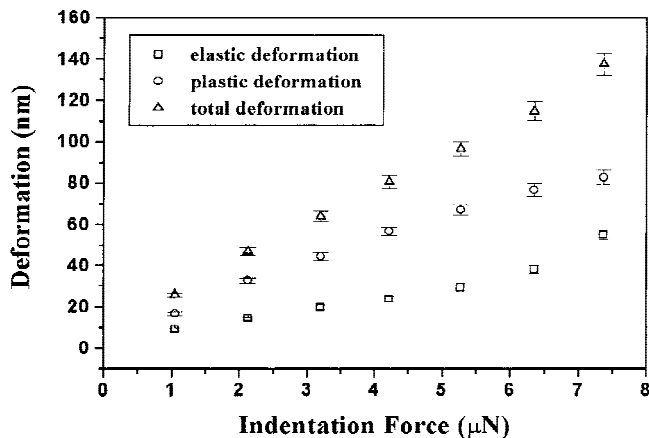


FIG. 5. Elastic, plastic, and total deformation of a PC thin film measured using AFM nanoindentation with the same diamond-tipped probe and the same seven contact forces as used for the nanoscratch tests of Fig. 3.

where  $(A_1 + A_2)$  is the cross-sectional area of the material pushed by plastic deformation to the groove edge, as shown in Fig. 3. Thus, the energetic wear rate  $K_e$  can be rewritten as

$$K_e = \frac{V}{fL} = \frac{f_{ab} A_v L}{fL} = \frac{f_{ab} A_v}{f}. \quad (3)$$

This fraction can be calculated using the AFM image data. Note, however, that the tip might be coated with polymer after scratching and that the same tip was used for both scratching and imaging, possibly creating experimental uncertainties. Also, friction and wear characteristics will depend on the tip-sample contact geometry during scratching rather than the geometry of the wear grooves imaged after scratching. Thus, elastic recovery during unloading and creep recovery over the time period between unloading and imaging will cause discrepancies between the cross-sectional areas measured from the AFM images of the scratches and those actually involved in the scratch process. Because no feedback is used during scratching, the probe simply moves laterally across the sample surface. In other words, no vertical adjustments are made such that the penetration depth of the tip remains essentially constant during scratch, even though the lateral forces alter the cantilever deflection. Therefore, a more accurate calculation of  $A_v$  can be obtained from the force plot recorded for nanoindentation with the same contact force, i.e., same penetration depth, as used in the scratch tests. In this case,  $A_v$  is calculated on the basis of the total penetration of the tip into the sample at the maximum indentation load using the idealized tip geometry shown in Fig. 6. The fraction  $f_{ab}$  was then calculated to be  $0.60 \pm 0.03$  (note that  $A_1$  and  $A_2$  were still measured from the cross-sectional profile), and the energetic wear rate  $K_e$  for the PC thin film was calculated to be  $0.94 \pm 0.05 \text{ mm}^3/(\text{N m})$ . From comparisons of the

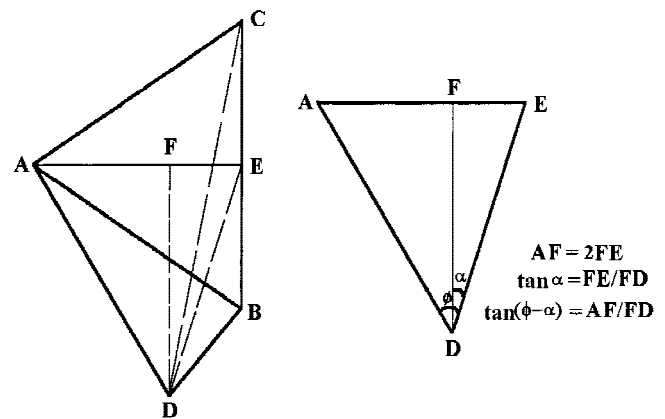


FIG. 6. Schematic of the ideal geometry for the triangular pyramidal diamond indenter tip. The apex angle of indenter,  $\phi$ , is about  $60^\circ$  and the half-included angle of indenter,  $\alpha$ , is about  $21.6^\circ$  (manufacturer specifications).

scratch depths shown in Fig. 3(b) with the total penetration depths shown in Fig. 5, calculations of  $K_e$  using the imaged scratch depths instead of the total penetration depths would underestimate the actual wear rate, particularly for the higher applied forces.

#### IV. SUMMARY

In summary, AFM force plots recorded during nanoscratch and nanoindentation tests were different with respect to the maximum force of unloading. On the basis of the quasi-static force equilibrium conditions, an analysis of the force plots recorded in nanoscratch tests was made for a scratch angle of  $0^\circ$ . This analysis was then used to compute the plowing friction for a polycarbonate thin film. The plowing friction was proportional to the contact force, allowing calculation of a coefficient of plowing friction for the diamond tip-PC system. Combining nanoscratch testing with nanoindentation testing, the energetic wear rate  $K_e$  of the sample was estimated.

#### ACKNOWLEDGMENTS

This work was supported by the National Science Foundation of China. The sapphire sample for calibrating the detection sensitivity of SFM was kindly supplied by Drs. S. Magonov and L. Huang of Digital Instruments.

Certain commercial instruments and materials are identified in this paper to adequately describe the experimental procedure. In no case does such identification imply recommendation or endorsement by the National Institute of Standards and Technology, nor does it imply that the instruments or materials are necessarily the best available for the purpose.

#### REFERENCES

1. B. Bhushan, J.N. Israelachvili, and U. Landman, *Nature* **374**, 607 (1995).
2. M. Kempf, M. Gen, and H. Vehoff, *Appl. Phys. A* **66**, S843 (1998).
3. M.R. VanLandingham, S.H. Mcknight, G.R. Palmese, J.R. Elings, X. Huang, T.A. Bogetti, R.F. Eduljee, and J.W. Gillespie, Jr., *J. Adhes.* **64**, 31 (1997).
4. W.C. Oliver and G.M. Pharr, *J. Mater. Res.* **7**, 1564 (1992).
5. S. Umemura, Y. Andoh, S. Hirono, T. Miyamoto, and R. Kaneko, *Philos. Mag. A* **74**, 1143 (1996).
6. E. Hamada and R. Kaneko, *J. Phys. D* **25**, A53 (1992).
7. E.V. Anokin, M.M. Yang, J.L. Chao, J.R. Elings, and D.W. Brown, *J. Vac. Sci. Technol. A* **16**, 1741 (1998).
8. A. Wiens, G. Persch-Schuy, M. Vogelgesang, and U. Hartmann, *Appl. Phys. Lett.* **75**, 1077 (1999).
9. F.N. Jones, W. Shen, S.M. Smith, Z. Huang, and R. Ryntz, *Prog. Org. Coat.* **34**, 119 (1998).
10. Digital Instruments Inc., Support Note No. 225, Rev. F, Santa Barbara, CA, 1998.
11. M.R. VanLandingham, *Microsc. Today* **97-10**, 12 (1997).
12. J.K. Lancaster, *Plast. Polym.* **41**, 297 (1973).